ACS Catalysis

pubs.acs.org/acscatalysis

Perspective

Dynamic Binuclear Cu^{II} Sites in the Reduction Half-Cycle of Low-Temperature NH_3–SCR over Cu-CHA Catalysts

Wenshuo Hu, Federica Gramigni, Nicole Daniela Nasello, Nicola Usberti, Umberto Iacobone, Shaojun Liu, Isabella Nova, Xiang Gao, and Enrico Tronconi*

Cite This: *ACS Catal.* 2022, 12, 5263–5274

Read Online

ABSTRACT: As the state-of-the-art catalyst for the selective catalytic reduction (SCR) of NOx from lean-burn engines, Cu-exchanged chabazite zeolite (Cu-CHA) has been a spotlight in environmental catalysis because of its preeminence in DeNOx performance and hydrothermal stability. The microscopic cycling of active Cu cations between Cu^{II} and Cu^{I} in response to dynamic, macroscopic reaction conditions dominates SCR catalysis over Cu-CHA zeolites. In such cycling, Cu cations are solvated by gas-phase reactants, e.g., NH_3, under low-temperature (LT) conditions, conferring peculiar mobility to Cu-NH_3 complexes and making them act as mobilized entities during LT-SCR turnovers. Such motions provide LT-SCR—a typical heterogeneous catalytic process—with homogeneous features over Cu-CHA, but, differently from conventional homogeneous catalysis, the motions are tethered by electrostatic interactions between Cu cations and conjugate Al centers. These features affect distinctly the LT-SCR redox chemistry on Cu-CHA, resulting in, for example, the involvement of two Cu^{I}-diamines in activating O_2 and reoxidizing Cu^{I} to Cu^{II} (oxidation half-cycle, OHC). The kinetically relevant reduction half-cycle (RHC) that reduces Cu^{II} to Cu^{I} is far less understood particularly within the context of such linked homo- and heterogeneous catalysis. Here, we focus on the LT-RHC chemistry over Cu-CHA and summarize observations from a series of recent, dedicated works from our group, benchmarking these findings against those closely relevant in the literature. We thus attempt to reconcile and rationalize results informed from independent, multitechnique evidence and to further progress mechanistic insights into LT-SCR catalysis, especially in the context of dynamic interconversion between mono- and binuclear Cu sites.

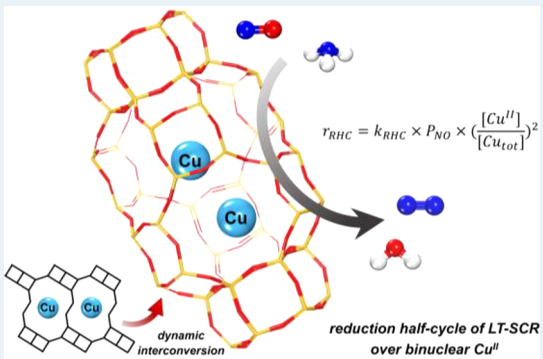

KEYWORDS: *Cu-CHA, NH_3–SCR, nitrogen oxides, low-temperature, redox mechanism*

1. INTRODUCTION

Cu-exchanged chabazite-type (Cu-CHA) zeolites are the state-of-the-art catalysts for the control of vehicular NOx emissions from lean-burn engines via selective catalytic reduction by NH_3 (NH_3–SCR). Their rapid commercial application as NH_3–SCR catalysts since a decade ago has been a major breakthrough in environmental catalysis. Cu-CHA zeolites exhibit salient low-temperature (LT, e.g., 473 K) DeNOx activity in SCR reactions, are hydrothermally stable up to high temperatures and are highly resistant to hydrocarbon poisoning because of their small micropore opening (3.8 Å × 3.8 Å).[1−4] These prominent catalytic performances, as well their simple, well-defined molecular structure, feature Cu-CHA as an ideal catalytic material for both fundamental and practical research. In particular, characterization of active sites in response to real, dynamic SCR working conditions and of elementary/pseudoelementary steps deciphering reaction mechanisms has been extensively conducted to reveal the catalytic chemistry underlying the preeminent LT-SCR activity of Cu-CHA. It is now established that NH_3–SCR reactions over Cu-CHA follow a redox mechanism involving reduction and reoxidation of Cu ions in two halves of the redox cycle, namely, $Cu^{II} \rightarrow Cu^{I}$ (reduction half-cycle, RHC) and $Cu^{I} \rightarrow Cu^{II}$ (oxidation half-cycle, OHC).[5−13] These Cu cations are found to be fully solvated by NH_3 under LT-SCR conditions, forming multiple Cu-NH_3 complexes as informed from reaction kinetic, in situ/operando spectroscopic, titrimetric measurements and simulation assessments from both kinetic modeling and first-principles calculations.[3,5−16] Such NH_3 solvation effects confer peculiar mobility to Cu-NH_3 complexes, liberate them from zeolite frameworks, and enable them to act as inter/intracage mobile entities during LT-SCR turnovers.[7,9,11−13,17,18] The intracrystallite motions of active centers are reminiscent of homogeneous catalytic reactions, but differ from the overarching tenet of conventional

Received: March 9, 2022
Revised: April 5, 2022
Published: April 18, 2022

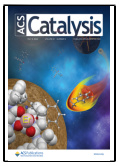

https://doi.org/10.1021/acscatal.2c01213
ACS Catal. 2022, 12, 5263–5274

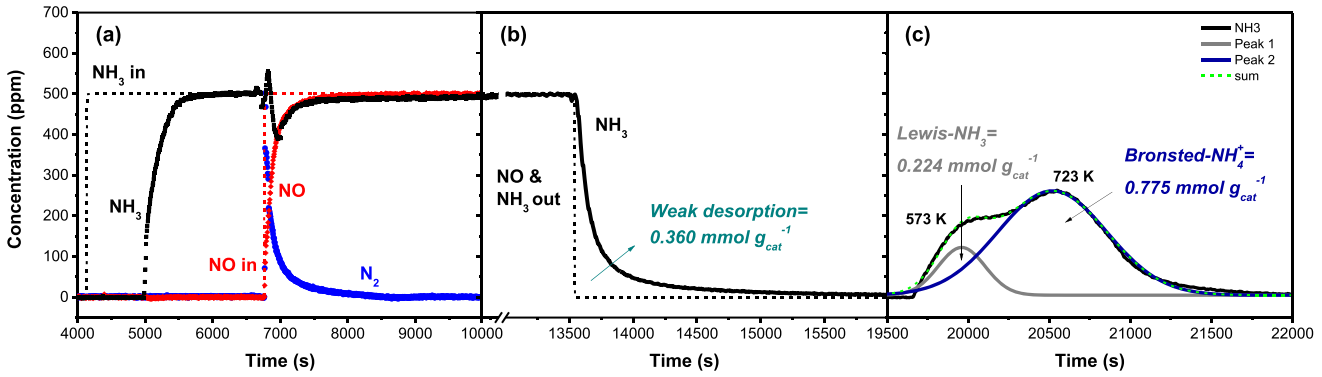

Figure 1. TRM test on preoxidized Cu-CHA (8% of O_2 at 823 K for 1 h) at T = 423 K and flow rate = 74 $cm^3\ s^{-1}\ g_{cat}^{-1}$ (STP): (a) reduction phase, NO = NH_3 = 500 ppm; before NO adding: O_2 = 8%, after: O_2 = 0% and (b) He purge. (c) TPD phase at 0.25 K s^{-1} from 423 to 823 K. Integral results and deconvolution of the TPD trace were reported in panel c. Adapted with permission from ref 12. Copyright 2021 Wiley.

homogeneous catalysis as their motions are tethered by electrostatic interactions between Cu cations and conjugate Al centers, which therefore reflects a distinct catalytic scenario that goes beyond conventional heterogeneous or homogeneous catalysis.[3,7,13,18]

Within this context, O_2 activation, a key step in LT−OHC that involves a four-electron transfer ($O_2 \rightarrow 2O^{2-}$), has been well accepted based on two linear Cu^I-diamine species to form binuclear Cu^{II}-oxo complexes through intercage diffusion, although such a scheme addresses the exchange of only two electrons ($2Cu^I \rightarrow 2Cu^{II}$), while the fate of the other two still remains debated.[8,11,13,17−19] The OHC process was suggested as kinetically relevant to the overall LT-SCR based on the second-order dependence of LT-SCR rates on Cu densities over low-loaded Cu-CHA catalysts and on changes in measured apparent activation energies with varying Cu loadings.[7,13,20] More recent studies that tried to dissect RHC and OHC from LT-SCR, however, reported controversial arguments based on operando spectroscopy and kinetic measurements and modeling: the kinetic relevance of RHC, OHC, and both have been proposed.[6,8,21] Such inconsistencies reflect also the lack of in-depth understanding of LT-RHC, as the related literature is far from consensus and diverges in terms of, for example, Cu^{II} speciation, reaction intermediates, and elementary steps. Most of the literature describes LT-RHC to be mediated by isolated Cu^{II}−NH_3 species through, for example, NO-assisted NH_3 activation to NH_2NO[9,22] or NO oxidative activation to HONO;[7,20,23] these single-site mechanisms would follow first-order dependence on Cu^{II}. Our group, however, for the first time reported the second-order dependence of LT-RHC rates on Cu^{II},[12,24,25] as also observed in a recent joint work from Oak Ridge National Laboratory and Cummins Inc.[6] Such quadratic kinetics strongly question single-site LT-RHC mechanisms and, instead, suggest a binuclear Cu^{II}-mediated pathway. These discussions are inextricably linked to the mechanistic understanding of LT-SCR, such as the identity of kinetically relevant steps and how to close the overall LT-SCR redox cycle, which would establish a foundation for the development of next generations of further improved SCR catalysts.

Here, we review systematic investigations that focus specifically on the LT-RHC chemistry over Cu-CHA. This Perspective summarizes observations from a series of recent publications made by our group[12,24−28] and benchmarks these findings against those closely relevant in the literature, with an attempt to reconcile and rationalize data, derivations and arguments reasoned from independent, multitechnique evidence, and eventually to further progress the mechanistic insights into LT-SCR catalysis. The recent advances in our works benefited from an integrated methodological framework coupling steady-state/transient kinetic, in situ/operando spectroscopic, chemical trapping/titrimetric and kinetic probe reaction experiments with theoretical treatments involving transient kinetic modeling and first-principles calculations. These investigations have been performed over industrially relevant Cu-CHA formulations (model catalysts from Johnson Matthey). We show that the speciation of Cu^{II} cations within Cu-CHA (ZCuOH and Z_2Cu) involved in LT-SCR can be both qualitatively and quantitatively characterized using simple, easily accessible transient response methods (TRM), which enable in situ assessment of Cu^{II} sites as a function of varying reaction conditions. By exposing NH_3-saturated Cu-CHA to reductive NO pulses, we reveal that NH_3 ligands coordinated to Cu^{II} cations are preferentially consumed in LT-RHC, prior to the NH_4^+ stored on Brønsted acid sites. The rates of such Cu^{II} reduction processes show a second-order dependence on Cu^{II}, regardless of Cu^{II} speciation, across a broad range of industrially relevant Cu-CHA samples and reaction conditions, which strongly question mechanisms based on isolated Cu^{II} cations but, instead, reflect a Cu^{II}-pair mediated LT-RHC pathway. These Cu^{II}-pairs are found to form in situ via concerting two separated but intercage mobile $Cu^{II}(OH)(NH_3)_x$ monomers originated from either initial ZCuOH populations or via facile hydrolysis of NH_3-ligated Z_2Cu, as probed by transient CO oxidation experiments and first-principles-derived thermodynamics and kinetics. These findings, along with the consequent mechanistic proposal of Cu^{II}-pairs catalyzed NO oxidative activation, reconcile satisfactorily a number of observations reported both in this paper and in the literature, and highlight the involvement of binuclear Cu^{II} species in LT-RHC as well. Such dynamic formation of binuclear Cu^{II} sites in both LT-RHC and LT−OHC enabled by NH_3 solvation consolidates the concept of peculiar, linked homo- and heterogeneous catalysis within the context of LT-SCR reactions over Cu-CHA zeolites; these may have the potential to be extended to mechanistic discussions on other SCR catalysts and to even other catalytic processes over similar zeolite materials (e.g., methane to methanol on Cu-CHA).

https://doi.org/10.1021/acscatal.2c01213
ACS Catal. 2022, 12, 5263−5274

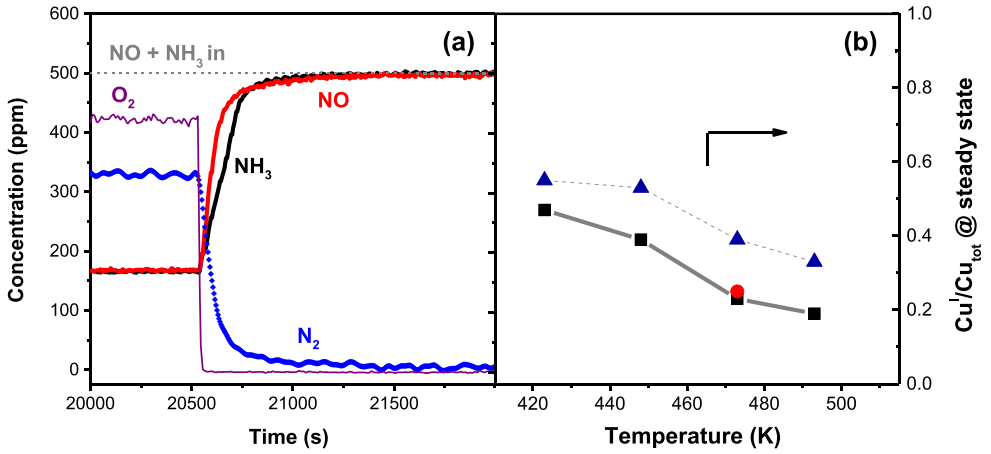

Figure 2. (a) TRM test starting from steady-state SCR at 473 K (with 2% H_2O) over Cu-CHA (the same sample as used above). (b) Measured Cu^I fractions by TRM experiments at different temperatures. Black squares (H_2O = 2%) and blue triangles (H_2O = 0%): data measured in this work; reaction conditions: NO = NH_3 = 500 ppm, O_2 = 8% (cutoff at ~20500 s in panel a), H_2O = 2% (when used), total flow rate = 125 $cm^3\ s^{-1}\ g_{cat}^{-1}$ (STP). Red circle: data measured by Deka et al., in the presence of 5% H_2O.[6]

2. RHC STOICHIOMETRY AND ITS KINETIC RELEVANCE

2.1. Stoichiometry of LT-RHC. The reduction half-cycle of LT-SCR reduces Cu^{II} to Cu^I by NO+NH_3 with N_2 and H_2O as the reaction products. This RHC process can be rigorously assessed using transient experiments (i.e., TRM), in which fully oxidized Cu-CHA is exposed to NO+NH_3 under isothermal conditions. Figure 1 illustrates a typical TRM test conducted at 423 K over a preoxidized representative model Cu-CHA catalyst (Cu = 1.7% wt., Si/Al = 12.5, Cu/Al = 0.24, from Johnson Matthey; majority of ZCuOH[9,12,26]) that was first saturated in NH_3+O_2. The addition of NO after O_2 cutoff resulted in an intense N_2 peak (~370 ppm), as displayed in Figure 1a, which progressively decreased to zero, with mirror-like NO consumption dynamics. Integral calculations estimate an overall N_2 production of 0.268 mmol g_{cat}^{-1} and NO conversion of 0.251 mmol g_{cat}^{-1}. These values are comparable, within the experimental error, to the Cu-loading of 0.278 mmol g_{cat}^{-1} and thus indicate almost complete Cu^{II} reduction during the NO+NH_3 transient. Such a complete Cu^{II} reduction by NO+NH_3 applies across a broad array of reaction conditions[24,25] and of Cu-CHA zeolites with different Cu loadings and Si/Al ratios,[26] as revealed by similar TRM experiments. Consistent with these, spectroscopic measurements, for example, UV−vis[8,12,29] and XANES,[9,22,30,31] collected under in situ/operando modes also provide supportive evidence, thus consolidating the observed Cu^{II} reduction chemistry. Further, cutting off NH_3 (and NO, Figure 1b) and measuring NH_3 release during subsequent temperature-programmed desorption (TPD, Figure 1c) at the end of NO+NH_3 transients provides direct, quantitative insights into the coordination environment of Cu^I. Deconvolution of the NH_3-TPD profile yields estimates of 0.224 mmol g_{cat}^{-1} for the LT-peak (~573 K, Lewis-NH_3 ligated to Cu^{I}[15,16,25,26,32]) and 0.775 mmol g_{cat}^{-1} for the high-temperature peak (~723 K, Brønsted-NH_4^+ from the zeolite framework[15,16,25,26,32]); adding weakly bound NH_3 (0.360 mmol g_{cat}^{-1}, Figure 1b) to Lewis-adsorbates, the former of which represents additional NH_3 molecules coordinated to Cu ions when gaseous NH_3 exists and solvates Cu, results in an NH_3/Cu ratio of ~2.1, thus strongly reflecting a two-NH_3-ligands structure—$Cu^I(NH_3)_2$—widely documented as the main Cu^I speciation in Cu-CHA catalyzed LT-SCR.[7−11,18,19,33,34] Given that the Brønsted-NH_4^+ remained unchanged with respect to the reference NH_3 adsorption + TPD analysis [Figure S1 of the Supporting Information (SI)] and that the number of NH_3 ligands decreased from ~3 (SI-S1) to ~2 (Figure 1), these results demonstrate the consumption of one NH_3 ligand in Cu^{II} reduction and further an equimolar LT-RHC stoichiometry of Cu:NO:NH_3:N_2 = 1:1:1:1, as observed also for different Cu-CHA catalysts and experimental reaction conditions.[8,24,25] These data, together with H_2O formation during the NO+NH_3 transient (Figure S2), confirm the reduction stoichiometry for Z_2Cu and ZCuOH (NH_3 is given in the form of independent reactants instead of ligands to better display the stoichiometry):

$$Cu^{II} + NO + NH_3 \rightarrow Cu^I + N_2 + H_2O + H^+ \quad (R.1)$$

$$Cu^{II}OH + NO + NH_3 \rightarrow Cu^I + N_2 + 2H_2O \quad (R.2)$$

2.2. Probing Cu Oxidation States Using TRM Tests. Such an established LT-RHC stoichiometry also enables a convenient quantitative assessment of average Cu oxidation states by titrating residual Cu^{II} with NO+NH_3, in complement to in situ/operando spectroscopies.[8−11,13,30,34] As an example, applying this method can estimate the average Cu^I and Cu^{II} fractions of the catalyst loading during steady-state LT-SCR reactions. As illustrated in Figure 2a, cutting off O_2 from the standard SCR feed stream resulted in a reductive phase of NO +NH_3, with NO and NH_3 progressively approaching their feed level while N_2 decreased to zero. This process reflects the reduction of residual Cu^{II} from steady-state LT-SCR; integration of NO consumption and N_2 formation upon O_2 cutoff gives 0.212 and 0.219 mmol g_{cat}^{-1}, respectively, which, according to the above stoichiometry, corresponds to ~23% of Cu^I present at 473 K steady-state SCR over this industrially relevant Cu-CHA sample (the same used in Figure 1). Performing the same test at different temperatures shows 20%−50% of Cu^I at steady-state SCR over the Cu-CHA sample used and in the low-temperature range tested here (423, 448, 473, 493 K, Figure 2b). Consistent with this, Deka et al.[6] used the same TRM protocol to estimate Cu^I fractions at steady-state SCR over a commercial washcoated honeycomb monolith Cu-CHA catalyst (Cu ~ 2.4% wt., Si/Al ~ 15) and

https://doi.org/10.1021/acscatal.2c01213
ACS Catal. 2022, 12, 5263−5274

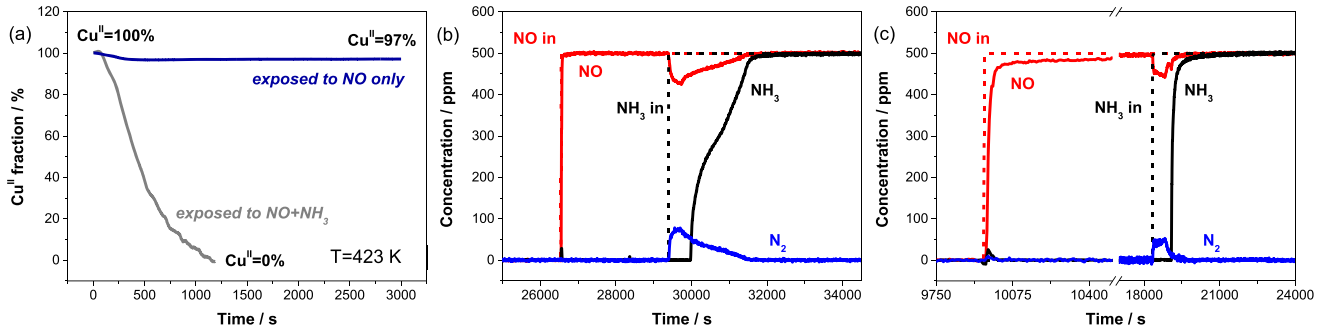

Figure 3. (a) Time-resolved operando UV−vis results (the wavelength at 793 nm was followed) over preoxidized Cu-CHA (the same sample as used above), NO = 1000 ppm, NH_3 = 1000 ppm (when used), O_2 = 0%; TRM tests over preoxidized (b) Cu-CHA and (c) mechanical mixture of Cu-CHA+BaO/Al_2O_3, NO = 500 ppm, NH_3 = 500 ppm (when used), O_2 = 0%. T = 423 K, flow rate = 125 $cm^3\ s^{-1}\ g_{cat}{}^{-1}$. Adapted with permission from ref 12. Copyright 2021 Wiley.

reported 25% of Cu^I at 473 K (red circle, Figure 2b), very similar to that in Figure 2 (23% at 473 K). Such a minority of Cu^I fractions reflect the kinetic relevance of RHC to the overall LT-SCR turnover. Besides, it is worth mentioning that generally higher Cu^I fractions are observed when H_2O is absent (Figure 2b), which suggests an inhibitory role of H_2O in LT-RHC.[24] The mechanistic interpretation of such H_2O effects is lacking and requires further exploration, as discussed in detail in Section 5.

Quantitative assessments of Cu^{II} and Cu^I fractions under LT-SCR conditions can also be obtained using in situ/operando XANES spectroscopy, as extensively documented in the literature in the past decade. The derived Cu^I fractions, however, seem unconverged. For example, Liu et al.[8] reported 20%−40% of Cu^I present during steady-state SCR at 423−473 K over a similar compositional Cu-CHA catalyst (Si/Al = 14. Cu/Al = 0.29); Lomachenko et al.[30] observed ∼46% of Cu^I at 423 K over Cu-CHA with Si/Al = 15 and Cu/Al = 0.48. These results are consistent with TRM estimations in Figure 2b, which suggest the minority of Cu^I in LT-SCR. However, different observations are also reported. On a low-loaded Cu-CHA sample (Si/Al = 14, Cu/Al = 0.17), Marberger et al.[10] observed a majority of Cu^I (>70%) at 463 K steady-state SCR, while Paolucci et al.[9] reported nearly internally identical Cu^{II}/Cu^I at 473 K over Cu-CHA zeolites with significantly different compositions (Si/Al = 15, Cu/Al = 0.44 and Si/Al = 5, Cu/Al = 0.08). The origin of such diversity is unclear for the moment but may result from the lumped, complex impacts from, for example, Cu-CHA structural differences as the consequence of different synthesis protocols,[3,9] different copper distributions among samples with different compositional parameters,[8,13] different reference compounds used for the linear combination fit of XANES spectra,[8,9,30] hydrodynamic and kinetic differences between operando reactor cells and plug-flow reactors,[9,10] and/or distinct reaction conditions adopted for in situ/operando measurements.[8−10,30]

3. INTERACTIONS OF Cu^{II} WITH RHC REACTANTS: NO AND NH_3

3.1. Cu^{II} Reduction by NO. As discussed above, Cu^{II} reduction proceeds to completion in the flow of NO+NH_3. It is thus necessary to examine independently the interactions of NO and NH_3 with Cu^{II} cations to dissect the reduction chemistry. Cu^{II} reduction by NO only is known to be limited at low temperatures, as widely documented using spectroscopic measurements[9,12,31,35−37] and theoretical calculations.[9,12,37,38] Figure 3 illustrates operando UV−vis spectroscopic and TRM titrimetric results, in which Cu^{II} reduction by NO only is rather limited according to both techniques: ∼3% of Cu^{II} reduction by UV−vis (Figure 3a) and ∼9% by the TRM test (Figure 3b), in which Cu-CHA was sequentially exposed to NO and NO+NH_3, with the latter step titrating residual Cu^{II} after NO exposure (additional details in SI-S3). Such a limited Cu^{II} reduction seems to reflect thermodynamic constraints on the weak interaction between Cu^{II} and NO, rather than originating from the inactive nature of the Cu^{II}+NO reaction chemistry. Indeed, hybrid functional (HSE06) DFT calculations reveal that NO alone does have the potential to reduce $Cu^{II}OH$ to Cu^I, with a gaseous nitrite-precursor intermediate, HONO, being the product of the reduction process (SI-S4). This NO + $Cu^{II}OH \leftrightarrow Cu^I$ + HONO reaction shows an endergonic Gibbs free energy of +12 kJ mol^{-1} (0.1 MPa, 423 K), thus also indicating a limited Cu^{II} reduction extent (∼15%). Along these lines, the presence of a HONO scavenger that can effectively consume HONO would enhance the Cu^{II} reduction extent through relieving thermodynamic constraints. This prediction was examined by mixing Cu-CHA with BaO/Al_2O_3, a NOx storage material that is able to store nitrites/nitrite-precursors in the form of $Ba(NO_2)_2$ with exothermic features.[39−43] Performing the same TRM test over the mechanical mixture of Cu-CHA+BaO/Al_2O_3 showed much more significant Cu^{II} reduction, that is, ∼41% of Cu^{II} reduction by NO only (Figure 3c). Additionally, performing a TPD measurement after exposing the Cu-CHA +BaO/Al_2O_3 mechanical mixture to NO showed a release of NOx at low temperatures typical of nitrites decomposition,[12,44,45] thus confirming the formation and storage of HONO, a nitrite precursor. These two results therefore validate the above argument based on promoted Cu^{II} reduction and promoted product formation, respectively.

Given that NH_3 is also able to react with nitrite species[7,19,20,23,40,44,46] and is in much closer contact with Cu^{II} than mechanically mixed BaO/Al_2O_3 powders, such a HONO scavenging effect is expected to be even more effective when NH_3 is copresent, consistent with the complete Cu^{II} reduction by NO+NH_3 discussed in Section 2.1 and with the operando UV−vis spectroscopy results in Figure 3a. Therefore, these experimental and theoretical observations converge in suggesting that NO oxidative activation to mobile nitrite-precursors is an eligible mechanism for the low-temperature Cu^{II} reduction, the extent of which is promoted by removal of the gaseous HONO product.[12]

https://doi.org/10.1021/acscatal.2c01213
ACS Catal. 2022, 12, 5263−5274

3.2. Catalytic Consequences of NH_3 Adsorption. It is now established that NH_3 significantly affects speciation, mobility and reactivity of Cu cations in Cu-CHA via adsorption and ligation.[9,10,12,25,47] At low temperatures, such NH_3 solvation liberates Cu cations from the zeolite framework and grants inter/intracage mobility to Cu-NH_3 complexes. Under LT-SCR conditions, Cu^{II} stays fully coordinated with NH_3 as $Cu^{II}(NH_3)_4$ and $Cu^{II}(OH)(NH_3)_3$, respectively, as informed from NH_3 isothermal adsorption + TPD analysis[12,26] (see also Figure S1), in situ/operando XAS assessments[8,9] and theoretical calculations.[9] In addition to these NH_3 ligands, that is, Lewis type NH_3-adsorbates (L-NH_3), NH_3 also adsorbs onto zeolite frameworks as Brønsted-type NH_4^+ (B-NH_4^+).

Reactivity of L-NH_3 and B-NH_4^+ and their contributions to SCR turnovers have been a long-standing debate in the SCR field.[2,48−56] In the case of Cu-CHA, various groups used in situ FTIR spectroscopy to examine LT reactivity of the two NH_3 adsorbates and reported consistent results that L-NH_3 is much more active than B-NH_4^+.[2,52−54] Deriving quantitative, kinetic information from IR spectra, however, requires rigorous assessments of extinction coefficients of L-NH_3 and B-NH_4^+,[49,57] which makes such attempts quite challenging. TPD analysis, on the other hand, can also distinguish L-NH_3 and B-NH_4^+ based on their distinct binding strengths.[15,16,26,32] Figure 4 displays a series of combined TRM + TPD experiments, which consist of six reductive pulses (Figure 4a, i.e., NO exposure at each t = 0−400 s) and five intervening oxidative pulses (8% of O_2, from last t = 400 s to the next t = 0 s). Since NH_3 was only preloaded once before the first NO pulse, these reductive-oxidative cycles reflect consumption of each NH_3 adsorbate during each reductive pulse, as assessed by subsequent TPD analysis (Figure 4b). During the first NO pulse (Figure 4a), prominent N_2 formation was observed, and the molar ratio of Cu:NO:N_2 was 1:1:1, consistent with the LT-RHC stoichiometry. The subsequent TPD profile (Figure 4b), when compared to an NH_3 isothermal adsorption + TPD reference test, reveals explicitly that only L-NH_3 was involved in this Cu^{II} reduction. Further reductive-oxidative cycles resulted in a progressive decrease in N_2 formation and consumption of B-NH_4^+, with the latter occurring only after the depletion of L-NH_3, which thus fully agrees with infrared spectroscopic observations. Further, the six reductive pulses were satisfactorily fitted by a redox kinetic model assuming NO activation by Cu^{II} to a gaseous mobile intermediate (HONO), which reacts first with L-NH_3 and then with B-NH_4^+.[25] Notably, the regressed turnover rates for consumption of L-NH_3 and B-NH_4^+ are equal, indicating their equivalent intrinsic reactivities; the preferential L-NH_3 consumption observed experimentally thus likely reflects its greater spatial proximity than B-NH_4^+ to the Cu^{II} active centers. Besides, this observation also rules out the NH_3-activation based mechanism[9,22] because B-NH_4^+ binding is much stronger;[9,15,16,25,26] thus, its desorption at 423 K to enable further activation on Cu^{II} active centers would be much slower than the observed Cu reduction rates.

4. DYNAMIC BINUCLEAR Cu^{II} SITES IN RHC

4.1. Transient Kinetic Analysis of Cu^{II} Reduction by NO+NH_3. As discussed in the Introduction, the detailed reaction mechanism underlying Cu^{II} reduction by NO+NH_3 is still under debate. A straightforward way to test these mechanistic proposals is to perform dedicated Cu^{II} reduction experiments (e.g., TRM tests like in Figure 1) and then

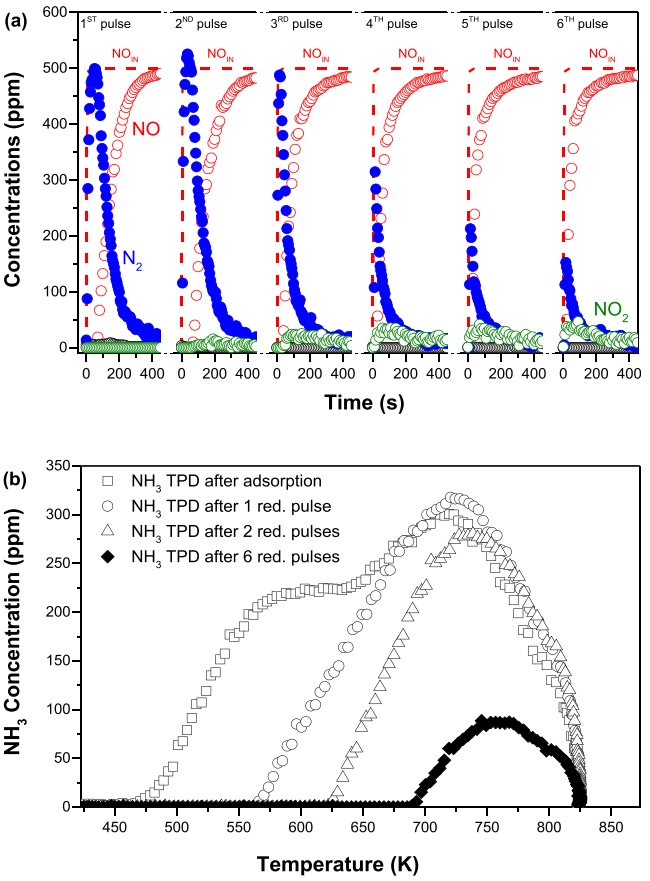

Figure 4. (a) Pulses of catalyst reduction with NO after preconditioning and NH_3 adsorption at 423 K. Feed composition: 500 ppm of NO in He. Reoxidation pulses (not shown) performed between NO reduction pulses. Feed composition: 8% of O_2 in He. (b) NH_3-TPD profiles of reference NH_3 isothermal adsorption + TPD (open squares), after the first (open circles), the second (open triangles) and the sixth reduction pulse with NO (solid diamonds). Feed composition: He. Flow rate: 74 $cm^3\ s^{-1}\ g_{cat}^{-1}$ (STP). Cu-CHA: the same sample as used above. Adapted with permission from ref 25. Copyright 2020 Elsevier.

benchmark mechanism-based kinetic models against experimental results. In doing so, a simplified global LT-RHC reaction that neglected Cu^{II} speciation was adopted (H_2O not balanced):[12,24,25]

$$2Cu^{II} + 2NO + 2NH_3 \rightarrow 2Cu^{I} + 2N_2 + H_2O \quad \text{(R.3)}$$

This reaction has equimolar stoichiometry (Cu:NO:NH_3:N_2 = 1:1:1:1) and thus reflects the LT-RHC chemistry and can describe Cu^{II} reduction in TRM tests. The TRM data were then fitted to a transient integral model of the test flow reactor, schematized as a cascade of 20 isothermal, isobaric Continuous Stirred Tank Reactors (CSTR). The turnover rate of Cu^{II} reduction is given by

$$r_{RHC} = k_{RHC} P_{NO} \left(\frac{Cu^{II}}{Cu_{tot}} \right)^n \quad (1)$$

where r_{RHC} and k_{RHC} are the turnover rate and the apparent rate constant for LT-RHC, respectively; P_{NO} is the partial pressure of NO; [Cu_{tot}] and [Cu^{II}] are the total loading and temporal amount of Cu^{II}, respectively. This rate equation is first-order in NO and zeroth-order in NH_3.[5,6] The kinetic

https://doi.org/10.1021/acscatal.2c01213
ACS Catal. 2022, 12, 5263−5274

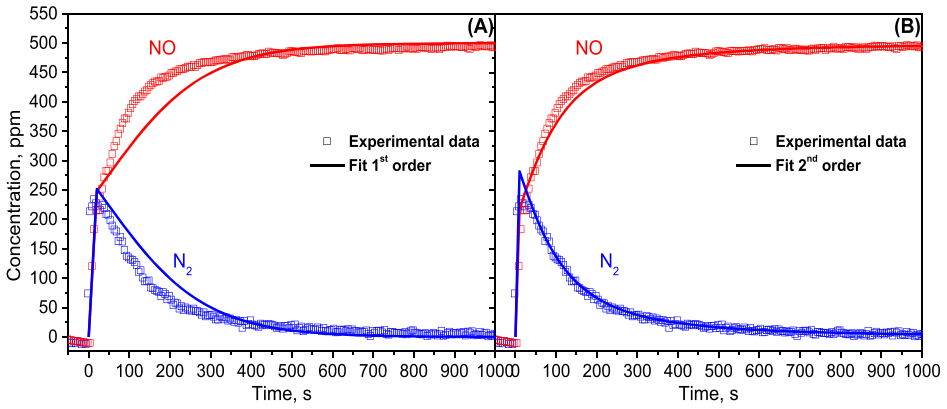

Figure 5. Experimental results (symbols) and kinetic fit (solid lines) over powdered Cu-CHA (the same sample as used above). Flow rate = 125 $cm^3\ s^{-1}\ g_{cat}^{-1}$ (STP), T = 423 K. Feed: NO = NH_3 = 500 ppm, H_2O = 0%. (A) First-order kinetic fit in Cu^{II}, (B) second order kinetic fit in Cu^{II}. Adapted with permission from ref 24. Copyright 2021 American Chemical Society.

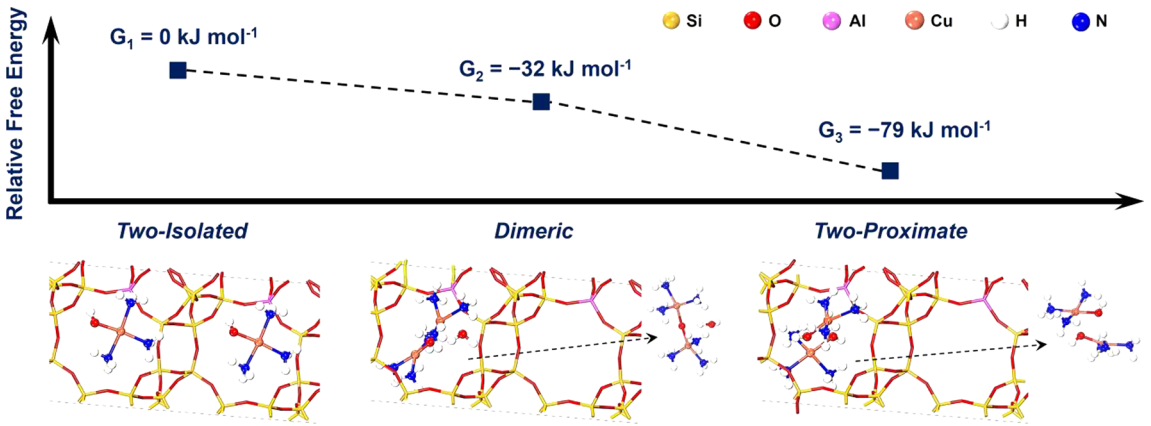

Figure 6. DFT-derived (HSE06+D3) Gibbs free energies of two-isolated (left), dimeric (central), and two-proximate (right) $Cu^{II}(OH)(NH_3)_3$. The free energies are referred to 0.1 MPa and 423 K. Adapted with permission from ref 12. Copyright 2021 Wiley.

dependence on Cu^{II} is set as an adjustable parameter (n = 1 or 2) determined by the data fit. Additional details on the kinetic model can be found in refs 12, 24.

Figure 5 reports a TRM test performed at 423 K over the same industrially relevant Cu-CHA catalyst but with a higher space velocity than that used in Figure 1. Assuming a first-order dependence on Cu^{II} (i.e., n = 1 in eq 1), although in line with popular LT-RHC mechanisms based on single-site Cu^{II}, failed to describe the dynamics of NO and N_2 concentrations (Figure 5a). In contrast, a successful fit was obtained by adopting a second-order dependence (i.e., n = 2 in eq 1). Such a satisfactory fit by quadratic kinetics was not occasional, but applied across a broad array of reaction temperatures (423−473 K), space velocities (e.g., the data in Figure 1a were also better fitted by the quadratic relationship[12]), NO feed concentrations and Cu-CHA zeolites (including commercial washcoated honeycomb monolith catalysts) under both dry and wet conditions (0% and 2% of H_2O, respectively; detailed in SI-S5).[6,12,24] These observations of a better fit with second-order kinetics in Cu^{II} than with first-order strongly question the proposed single-site LT-RHC mechanisms based on mononuclear Cu^{II} sites, reflecting, instead, an involvement of two Cu^{II} ions in LT-RHC catalysis, in analogy with the well-accepted binuclear LT−OHC pathway. Further, Cu-CHA catalyst samples dominated respectively by Z_2Cu and by ZCuOH showed identical kinetic responses during transient NO+NH_3 reduction, as revealed by running the same TRM tests over Cu-CHA samples with distinct Z_2Cu/ZCuOH ratios.[24,28] Such findings indicate that the two Cu^{II} sites are kinetically equivalent in mediating LT-RHC, although ZCuOH has been reported to be more reducible than Z_2Cu.[2,58−60]

4.2. Probing Binuclear Cu^{II} Sites under LT-RHC Conditions. A binuclear LT-RHC mechanism requires intercage diffusion of isolated Cu^{II}−NH_3 complexes and their subsequent pairing to form dual-site Cu^{II} active species. These two requirements are well met in the context of LT−OHC because its transportation medium $Cu^{I}(NH_3)_2$ is highly mobile, particularly in terms of intercage transportation,[13,17,18] and the combination of two $Cu^{I}(NH_3)_2$ with one O_2 molecule is exothermic,[13,17] which acts as a thermodynamic driving force to favor the pairing process. Similar assessments were also conducted for $Cu^{II}(OH)(NH_3)_3$, (i.e., the form of ZCuOH in LT-SCR conditions).[12] Figure 6 illustrates HSE06+D3 derived free energies of three possible configurations of $Cu^{II}(OH)(NH_3)_3$; those having two $Cu^{II}(OH)(NH_3)_3$ units in the same cage (central and right panels) are energetically more favorable than the isolated one (left panel). Such a stabilization of dual-site configurations results from their larger volumes than Cu^{II}-monomers, which originates stronger van der Waals interaction with the zeolite framework.[12] While $Cu^{II}(OH)(NH_3)_3$ is only intracage mobile and cannot diffuse through CHA cages according to AIMD simulations,[9] $Cu^{II}(OH)(NH_3)$ is only 3 kJ mol^{-1} less stable and has a low diffusion barrier of 12 kJ mol^{-1};[9,12] thus, it can serve as a proper transportation medium

https://doi.org/10.1021/acscatal.2c01213
ACS Catal. 2022, 12, 5263−5274

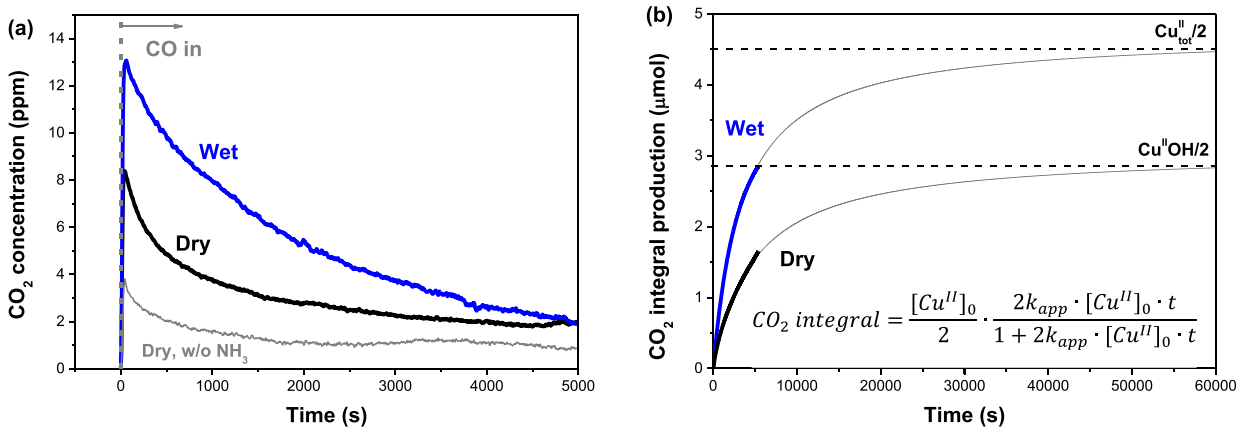

Figure 7. Transient CO oxidation tests over preoxidized Cu-CHA (the same sample as used above) with preadsorbed NH_3 (not shown): dry (black) vs wet (blue); without preadsorbed NH_3: dry (gray, panel a). Thin lines in panel b: model predictions from the inset equation; thick lines: experimental CO_2 integral production. Reaction conditions: T = 473 K, CO = 1000 ppm, O_2 = 0%, H_2O = 5% (for the wet test), and total flow rate = 74 $cm^3\ s^{-1}\ g_{cat}^{-1}$ (STP). Adapted with permission from ref 28. Copyright 2021 American Chemical Society.

in the LT-RHC case. These results suggest that $Cu^{II}(OH)(NH_3)_3$ also complies with the two requirements discussed above: two such species cohabiting the same cage is both thermodynamically and kinetically favorable, which thus renders theoretical support to the quadratic kinetics observed experimentally. Accommodation of additional $Cu^{II}(OH)(NH_3)_3$ is less favorable, indicating that dual-site configurations prevail over those with higher nuclearity.[12] Noteworthy, the configuration with two proximate $Cu^{II}(OH)(NH_3)_3$ (*Two-P*) is energetically more stable than a real Cu^{II}-μ-oxo dimer (Figure 6); a similar observation was also reported for $Cu^{II}(OH)(NH_3)_2$, a two-NH_3-ligand configuration.[7] This is compatible with the fact that *Two-P* is indeed a hydrolyzed product of the dimer and that H_2O is prevalent in exhaust gas and also forms as an SCR product.

In order to challenge the theoretical prediction of predominance of binuclear $Cu^{II}(OH)(NH_3)_3$, a probe reaction, that is, CO oxidation, was used to assess their existence. In fact, CO oxidation is known as a two-electron-transfer event[27,28,61,62] and thus requires the involvement of Cu^{II} pairs. Exposing preoxidized Cu-CHA to CO (Figure 7a, thin gray line) only led to limited CO_2 formation, suggesting a majority of isolated Cu^{II} cations within "clean" Cu-CHA; preloading NH_3, however, promoted CO_2 formation remarkably (Figure 7a, black line), and the CO_2 dynamics were accurately described by a quadratic rate expression: $r_{CO_2} = k_{app}\cdot[Cu^{II}]^2$, as illustrated in Figure 7b by the consistency between experimental CO_2 formation and integral second-order model predictions. Further, the asymptotic limit is equal to half the amount of ZCuOH in the tested Cu-CHA catalyst, reflecting that only ZCuOH is active in the Cu-dimer-mediated CO oxidation chemistry, in line with in situ UV−vis results.[27,28,62,63] These observations demonstrate the participation of two $Cu^{II}OH$ in CO oxidation and further the enhanced mobility of ZCuOH conferred by NH_3-ligands, which promotes CO oxidation by favoring the formation of paired Cu^{II}−NH_3 complexes.[12,27,28] The latter derivation is fully consistent with the theoretical results in Figure 6, therefore experimentally rationalizing the formation of binuclear $Cu^{II}OH$ structures under LT-SCR conditions.

Note that Z_2Cu is inactive in dry CO oxidation,[27,28,62,63] and this likely reflects its inability in forming Cu^{II} pairs needed for CO oxidation, as NH_3-solvated Z_2Cu (dual charge) clusters cannot diffuse through CHA cages because of stronger electrostatic tethering from the zeolite framework in comparison with single charge ZCuOH.[9,13] Z_2Cu, however, exhibits identical activity to ZCuOH in Cu^{II} reduction by NO +NH_3 and shows also quadratic kinetics, as aforementioned, which highlights the involvement of two Z_2Cu in LT-RHC reactions. Reconciling such a divergence requires to account for the dynamic interconversion between ZCuOH and Z_2Cu. As displayed in Figure 7a, adding H_2O to the gas stream promoted CO_2 formation distinctly (blue line); the "wet" CO_2 formation dynamics can again be nicely captured by the same second-order integral model, the asymptotic limit being now equal to half the total Cu loading (Figure 7b). This result indicates a promotional effect of H_2O on CO oxidation, and that H_2O "activates" Z_2Cu and enables it to intercage diffuse to form Cu^{II} pairs. Given that H_2O is prevalent in LT-SCR reactions, a similar promotional effect is expected to apply to LT-SCR as well. Indeed, a coupled in situ FTIR spectroscopic and theoretical investigation validated this hypothesis and revealed that Z_2Cu can be facilely hydrolyzed to ZCuOH in the presence of NH_3 via $Cu^{II}(NH_3)_4 + H_2O \rightarrow Cu^{II}(OH)(NH_3)_3 + NH_4^+$, both thermodynamically and kinetically favorable in the presence of subsequent scavenging reactions like CO oxidation and LT-RHC, so that Z_2Cu may eventually participate in LT-RHC under the actual form of ZCuOH.[28]

4.3. Binuclear Cu^{II}-Mediated LT-RHC Pathway. Given the above experimental, kinetic, and theoretical evidence, a LT-RHC pathway should comply with the stoichiometry of Cu:NO:NH_3:N_2 = 1:1:1:1, the second-order kinetics in Cu^{II}, the equivalent kinetic responses of Z_2Cu and ZCuOH, and the preferential depletion of L-NH_3 followed by B-NH_4^+ but with identical intrinsic activity. As discussed in Section 4.1, a first-order kinetic model based on single-site LT-RHC mechanisms[7,9,22,23,31,34] failed to describe the dynamics of TRM experiments; the Cu-dimer-based LT-SCR redox cycle proposed by Chen et al.[19] is compatible with the dual-site kinetic requirement, but in this mechanism, gaseous NH_3 reacts with activated NO through the assistance of Brønsted acid sites, which does not incorporate the catalytic role of L-NH_3. Considering the intercage mobility of NH_3-ligated ZCuOH, the facile conversion of Z_2Cu to ZCuOH via NH_3-assisted hydrolysis, and the DFT-derived *Two-P* configuration (Figure 6), a binuclear-$Cu^{II}OH$ (i.e., *Two-P*) mediated,

https://doi.org/10.1021/acscatal.2c01213
ACS Catal. 2022, 12, 5263−5274

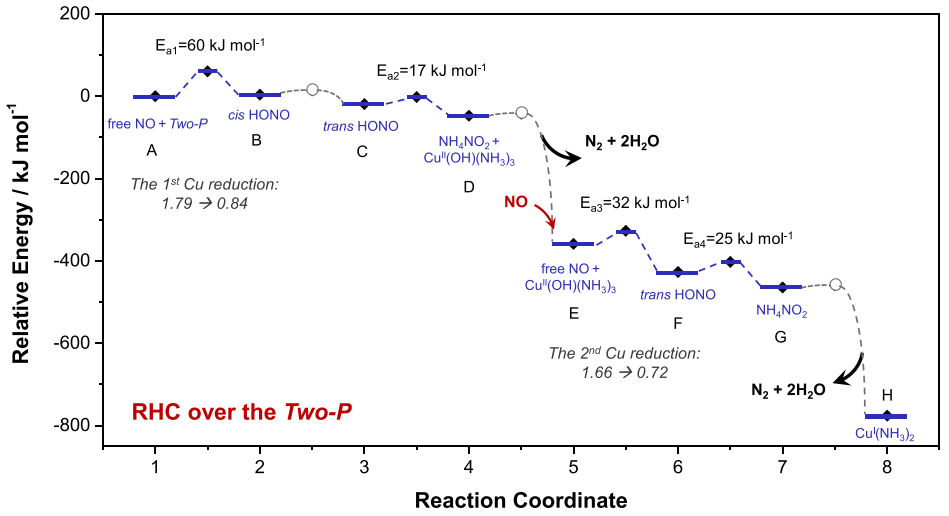

Figure 8. DFT-computed (HSE06+D3) energy landscape of LT-RHC over the *Two-P*. Activation energies and Cu^{II} reduction are reported. A → B: (R.4); B → C: facile isomerization of *cis*-HONO to *trans*-HONO; C → D: (R.5); D → E: (R.6); E → F: (R.7); F → G: (R.8); G → H: (R.9). Structures of A to H are provided in SI-S6. Adapted with permission from ref 12. Copyright 2021 Wiley.

HONO-based LT-RHC mechanism was proposed,[12] as illustrated in Figure 8. This mechanism consists of two sequential NO oxidative activation processes, each including three main steps: NO oxidative activation to HONO catalyzed by one $Cu^{II}(OH)(NH_3)_3$ unit (concurrently reducing Cu^{II} to Cu^{I}), HONO reacting with one NH_3 ligand to NH_4NO_2, and NH_4NO_2 decomposition to N_2 and H_2O, as illustrated in R.4−R.9:

$$NO + [Cu^{II}(OH)(NH_3)_3\cdots Cu^{II}(OH)(NH_3)_3] \rightarrow HONO + Cu^{I}(NH_3)_3 + Cu^{II}(OH)(NH_3)_3 \quad (R.4)$$

$$HONO + Cu^{I}(NH_3)_3 \rightarrow Cu^{I}(NH_3)_2 + NH_4NO_2 \quad (R.5)$$

$$NH_4NO_2 \rightarrow N_2 + 2H_2O \quad (R.6)$$

$$NO + Cu^{II}(OH)(NH_3)_3 \rightarrow HONO + Cu^{I}(NH_3)_3 \quad (R.7)$$

$$HONO + Cu^{I}(NH_3)_3 \rightarrow Cu^{I}(NH_3)_2 + NH_4NO_2 \quad (R.8)$$

$$NH_4NO_2 \rightarrow N_2 + 2H_2O \quad (R.9)$$

in which $[Cu^{II}(OH)(NH_3)_3\cdots Cu^{II}(OH)(NH_3)_3]$ stands for the *Two-P*. Summing these six steps results in the global reaction:

$$2NO + [Cu^{II}(OH)(NH_3)_3\cdots Cu^{II}(OH)(NH_3)_3] \rightarrow 2Cu^{I}(NH_3)_2 + 2N_2 + 4H_2O \quad (R.10)$$

consistent with the stoichiometry of $Cu:NO:NH_3:N_2$ = 1:1:1:1 and the molar ratio of H_2O/N_2 = 2 upon cutting off O_2.[28] Further, NO oxidative activation over the *Two-P* (R.4, A → B in Figure 8) has the highest activation barrier (+60 kJ mol^{-1}) and thus serves as the rate-determining step in the proposed cascade. Considering also the dynamic equilibrium between two isolated $Cu^{II}(OH)(NH_3)_3$ and the *Two-P*, the overall LT-RHC rate expression is derived as[12]

$$r_{RHC} = k_{app}P_{NO}\left[\frac{Cu^{II}(OH)(NH_3)_3}{Cu_{tot}}\right]^2 \quad (2)$$

where k_{app} is the apparent rate constant for the LT-RHC scheme in Figure 8, consistent with the quadratic kinetics observed experimentally. Since HONO is able to react facilely with both L-NH_3 and B-NH_4^+, and both reactions are kinetically irrelevant,[12,19] this mechanism is also compatible with the identical intrinsic activity of the two NH_3 adsorbates, although L-NH_3 is preferentially depleted because of its spatial proximity. NO oxidation to NO_2 is in principle also compatible with these experimental observations but is energetically less favorable because of the highly endothermic desorption of NO_2.[12] Note that the activation barrier for NH_3-assisted hydrolysis of Z_2Cu to ZCuOH is ~66 kJ mol^{-1},[28] comparable to that of the *Two-P*-based LT-RHC pathway; such a similarity suggests that the hydrolysis reaction proceeds in parallel to LT-RHC, so that they are kinetically indistinguishable and thus explain the identical apparent LT-RHC dynamics regardless of the initial $ZCuOH/Z_2Cu$ ratios. Accordingly, the proposed *Two-P*-based binuclear LT-RHC mechanism complies with all these experimental, kinetic and theoretical requirements. Further, such a binuclear LT-RHC pathway is also favorable in terms of the overall LT-SCR redox cycle because, as discussed in the Introduction, the LT−OHC is accepted to occur over dimeric Cu-oxo species; if binuclear structures are able to directly launch the RHC, there is no need to send back one of the Cu^{II}−NH_3 units to reestablish their original isolated state at the end of LT−OHC, especially since the latter configuration is thermodynamically less favorable.

5. SUMMARY AND OUTLOOK

This Perspective focuses on the LT-RHC of the SCR catalytic chemistry over Cu-CHA zeolites: it summarizes findings reported in a series of recent works from our group and benchmarks them against those closely relevant in the literature. Such a summary highlights the essential role of dynamic interconversion between mono- and binuclear Cu species not only in LT−OHC but also in LT-RHC, as enabled by their intracrystallite mobility conferred by NH_3 solvation. This, in turn, results in a peculiar catalytic landscape that links homo- and heterogeneous catalysis, a concept that had been put forth for the mechanistic interpretation of LT−OHC[7,13] but has also been demonstrated by us to be applicable and

https://doi.org/10.1021/acscatal.2c01213
ACS Catal. 2022, 12, 5263−5274

indispensable for rationalizing LT-RHC. Such strong interactions between gas-phase reactants and catalyst active centers in response to varying reaction conditions and external stimuli, as well their significant consequences for catalysis turnovers, are prevalent among different heterogeneous catalytic processes. The discussions and tenets delivered in this Perspective may have potential to be extended to interrogations of the SCR reaction chemistry over other catalysts and even to other processes catalyzed by similar zeolitic materials, including, for example, the eye-catching partial oxidation of methane to methanol on Cu-CHA catalysts.[3,9,64−69]

In spite of these progresses, however, several issues still remain unsettled in our view and need further interrogations. These include, but are not limited to, direct experimental measurements of mobility of Cu-NH_3 complexes. Experimental techniques such as impedance spectroscopy and solid-state nuclear magnetic resonance (NMR) spectroscopy have been used to investigate the mobility of $Cu^I(NH_3)_2$ in LT−OHC over Cu-zeolites[70,71] and of protons within H-ZSM-5 after interacting with H_2O,[72] respectively; applying these methods would be promising to provide direct experimental insights into intracrystalline motions of Cu^{II}, too. Additionally, the H_2O effect on LT-SCR turnovers is unclear, although the general understanding that H_2O seems to not affect significantly steady-state LT-SCR apparent kinetics. The measured average Cu oxidation states at steady-state LT-SCR (Figure 2b), in fact, show decreased Cu^I fractions when H_2O is present. Such an observation reflects the inhibitory effect of H_2O on LT-RHC, as also confirmed directly by the decreased LT-RHC rate constants in the presence of H_2O although their transient RHC kinetics still follow quadratic relationships.[24] Further, the apparent activation energy of LT-RHC under "wet" conditions decreased to about half of its "dry" counterpart (~60 kJ mol^{-1} to ~30 kJ mol^{-1}), which seems to suggest the involvement of additional exothermic equilibria when H_2O is present.[24] Given the limited effect of H_2O on overall LT-SCR kinetics, there appears to be also some promotion to LT−OHC by H_2O that can counterbalance its negative impact on LT-RHC, as supported by preliminary kinetic explorations.[24] Detailed mechanistic interpretations of such H_2O effects are still lacking but necessary, as percentage levels of moisture prevail in realistic exhausts. Achieving this goal also requires a clear understanding of how to close the LT-SCR redox cycle, that is, how to digest the remaining two electrons after activating one O_2 molecule by two Cu^I-diamine motifs, how to link the binuclear mediated LT−OHC with LT-RHC, etc. In addition to these discussions on SCR reactions that convert NO to N_2, another unwanted side product, N_2O, has now garnered more and more attention due to its high global warming potential. It is suggested that the low-temperature N_2O formation proceeds in the RHC and is favored by high Cu-CHA oxidation states,[73−79] but its mechanism is still unclear and remains debated. While further efforts are needed to resolve all the mechanistic puzzles of the RHC in LT NH_3−SCR, we believe that the present discussions may contribute a consistent framework to such endeavors.

■ ASSOCIATED CONTENT

Supporting Information

The Supporting Information is available free of charge at https://pubs.acs.org/doi/10.1021/acscatal.2c01213.

Additional experimental results regarding the speciation of Cu^{II}−NH_3 and the stoichiometry of LT-RHC, modeling results of transient kinetic analysis and DFT optimized structures (PDF)

■ AUTHOR INFORMATION

Corresponding Author

Enrico Tronconi − *Laboratory of Catalysis and Catalytic Processes, Dipartimento di Energia, Politecnico di Milano, 20156 Milano, Italy;* orcid.org/0000-0002-5472-2696; Phone: +39 02 23993264; Email: enrico.tronconi@polimi.it

Authors

Wenshuo Hu − *State Key Laboratory of Clean Energy Utilization, Zhejiang University, Hangzhou 310027, China;* Present Address: W.H.: Department of Chemical & Biomolecular Engineering, University of California at Berkeley, Berkeley, California 94720, United States; orcid.org/0000-0001-8280-1167

Federica Gramigni − *Laboratory of Catalysis and Catalytic Processes, Dipartimento di Energia, Politecnico di Milano, 20156 Milano, Italy*

Nicole Daniela Nasello − *Laboratory of Catalysis and Catalytic Processes, Dipartimento di Energia, Politecnico di Milano, 20156 Milano, Italy*

Nicola Usberti − *Laboratory of Catalysis and Catalytic Processes, Dipartimento di Energia, Politecnico di Milano, 20156 Milano, Italy*

Umberto Iacobone − *Laboratory of Catalysis and Catalytic Processes, Dipartimento di Energia, Politecnico di Milano, 20156 Milano, Italy*

Shaojun Liu − *State Key Laboratory of Clean Energy Utilization, Zhejiang University, Hangzhou 310027, China;* orcid.org/0000-0003-0976-5707

Isabella Nova − *Laboratory of Catalysis and Catalytic Processes, Dipartimento di Energia, Politecnico di Milano, 20156 Milano, Italy;* orcid.org/0000-0001-7239-2785

Xiang Gao − *State Key Laboratory of Clean Energy Utilization, Zhejiang University, Hangzhou 310027, China;* orcid.org/0000-0002-1732-2132

Complete contact information is available at: https://pubs.acs.org/10.1021/acscatal.2c01213

Notes

The authors declare no competing financial interest.

■ ACKNOWLEDGMENTS

Authors from Zhejiang University acknowledge the financial support from National Natural Science Foundation of China (51836006, 52006192).

■ REFERENCES

(1) Lambert, C. K. Perspective on SCR NOx control for diesel vehicles. *React. Chem. Eng.* **2019**, *4* (6), 969−974.

(2) Gao, F.; Kwak, J. H.; Szanyi, J.; Peden, C. H. F. Current Understanding of Cu-Exchanged Chabazite Molecular Sieves for Use as Commercial Diesel Engine DeNOx Catalysts. *Top. Catal.* **2013**, *56* (15−17), 1441−1459.

(3) Borfecchia, E.; Beato, P.; Svelle, S.; Olsbye, U.; Lamberti, C.; Bordiga, S. Cu-CHA−a model system for applied selective redox catalysis. *Chem. Soc. Rev.* **2018**, *47* (22), 8097−8133.

(4) Beale, A. M.; Gao, F.; Lezcano-Gonzalez, I.; Peden, C. H.; Szanyi, J. Recent advances in automotive catalysis for NOx emission control by small-pore microporous materials. *Chem. Soc. Rev.* **2015**, *44* (20), 7371−405.
(5) Partridge, W. P.; Joshi, S. Y.; Pihl, J. A.; Currier, N. W. New operando method for quantifying the relative half-cycle rates of the NO SCR redox cycle over Cu-exchanged zeolites. *Appl. Catal., B* **2018**, *236*, 195−204.
(6) Deka, D. J.; Daya, R.; Ladshaw, A.; Joshi, S. Y.; Partridge, W. P. A Transient-Response Methodology based on Experiments and Modeling for Cu-Redox Half-Cycle Kinetic Analysis on a Cu-SSZ-13 SCR Catalyst. *Chem. Eng. J.* **2022**, *435*, 134219.
(7) Gao, F.; Mei, D.; Wang, Y.; Szanyi, J.; Peden, C. H. Selective Catalytic Reduction over Cu/SSZ-13: Linking Homo- and Heterogeneous Catalysis. *J. Am. Chem. Soc.* **2017**, *139* (13), 4935−4942.
(8) Liu, C.; Kubota, H.; Amada, T.; Kon, K.; Toyao, T.; Maeno, Z.; Ueda, K.; Ohyama, J.; Satsuma, A.; Tanigawa, T.; Tsunoji, N.; Sano, T.; Shimizu, K. i. In Situ Spectroscopic Studies on the Redox Cycle of NH_3−SCR over Cu−CHA Zeolites. *ChemCatChem.* **2020**, *12* (11), 3050−3059.
(9) Paolucci, C.; Parekh, A. A.; Khurana, I.; Di Iorio, J. R.; Li, H.; Albarracin Caballero, J. D.; Shih, A. J.; Anggara, T.; Delgass, W. N.; Miller, J. T.; Ribeiro, F. H.; Gounder, R.; Schneider, W. F. Catalysis in a Cage: Condition-Dependent Speciation and Dynamics of Exchanged Cu Cations in SSZ-13 Zeolites. *J. Am. Chem. Soc.* **2016**, *138* (18), 6028−48.
(10) Marberger, A.; Petrov, A. W.; Steiger, P.; Elsener, M.; Krocher, O.; Nachtegaal, M.; Ferri, D. Time-resolved copper speciation during selective catalytic reduction of NO on Cu-SSZ-13. *Nat. Catal.* **2018**, *1* (3), 221−227.
(11) Negri, C.; Selleri, T.; Borfecchia, E.; Martini, A.; Lomachenko, K. A.; Janssens, T. V. W.; Cutini, M.; Bordiga, S.; Berlier, G. Structure and Reactivity of Oxygen-Bridged Diamino Dicopper(II) Complexes in Cu-Ion-Exchanged Chabazite Catalyst for NH_3-Mediated Selective Catalytic Reduction. *J. Am. Chem. Soc.* **2020**, *142* (37), 15884−15896.
(12) Hu, W.; Selleri, T.; Gramigni, F.; Fenes, E.; Rout, K. R.; Liu, S.; Nova, I.; Chen; Gao, X.; Tronconi, E. On the Redox Mechanism of Low-Temperature NH_3-SCR over Cu-CHA: A Combined Experimental and Theoretical Study of the Reduction Half Cycle. *Angew. Chem., Int. Ed.* **2021**, *60* (13), 7197−7204.
(13) Paolucci, C.; Khurana, I.; Parekh, A. A.; Li, S.; Shih, A. J.; Li, H.; Di Iorio, J. R.; Albarracin-Caballero, J. D.; Yezerets, A.; Miller, J. T.; Delgass, W. N.; Ribeiro, F. H.; Schneider, W. F.; Gounder, R. Dynamic multinuclear sites formed by mobilized copper ions in NOx selective catalytic reduction. *Science* **2017**, *357* (6354), 898−903.
(14) Wang, A.; Chen, Y.; Walter, E. D.; Washton, N. M.; Mei, D.; Varga, T.; Wang, Y.; Szanyi, J.; Wang, Y.; Peden, C. H. F.; Gao, F. Unraveling the mysterious failure of Cu/SAPO-34 selective catalytic reduction catalysts. *Nat. Commun.* **2019**, *10* (1), 1137.
(15) Daya, R.; Trandal, D.; Dadi, R. K.; Li, H.; Joshi, S. Y.; Luo, J.; Kumar, A.; Yezerets, A. Kinetics and thermodynamics of ammonia solvation on Z_2Cu, ZCuOH and ZCu sites in Cu-SSZ-13−Implications for hydrothermal aging. *Appl. Catal., B* **2021**, *297*, 120444.
(16) Daya, R.; Joshi, S. Y.; Luo, J. Y.; Dadi, R. K.; Currier, N. W.; Yezerets, A. On kinetic modeling of change in active sites upon hydrothermal aging of Cu-SSZ-13. *Appl. Catal., B* **2020**, *263*, 118368.
(17) Chen, L.; Falsig, H.; Janssens, T. V. W.; Gronbeck, H. Activation of oxygen on $(NH_3\text{-}Cu\text{-}NH_3)^+$ in NH_3-SCR over Cu-CHA. *J. Catal.* **2018**, *358*, 179−186.
(18) Millan, R.; Cnudde, P.; van Speybroeck, V.; Boronat, M. Mobility and Reactivity of Cu^+ Species in Cu-CHA Catalysts under NH_3-SCR-NOx Reaction Conditions: Insights from AIMD Simulations. *JACS Au* **2021**, *1* (10), 1778−1787.
(19) Chen, L.; Janssens, T. V. W.; Vennestrøm, P. N. R.; Jansson, J.; Skoglundh, M.; Grönbeck, H. A Complete Multisite Reaction Mechanism for Low-Temperature NH_3-SCR over Cu-CHA. *ACS Catal.* **2020**, *10* (10), 5646−5656.
(20) Gao, F.; Walter, E. D.; Kollar, M.; Wang, Y.; Szanyi, J.; Peden, C. H. F. Understanding ammonia selective catalytic reduction kinetics over Cu/SSZ-13 from motion of the Cu ions. *J. Catal.* **2014**, *319*, 1−14.
(21) Jones, C. B.; Khurana, I.; Krishna, S. H.; Shih, A. J.; Delgass, W. N.; Miller, J. T.; Ribeiro, F. H.; Schneider, W. F.; Gounder, R. Effects of dioxygen pressure on rates of NOx selective catalytic reduction with NH_3 on Cu-CHA zeolites. *J. Catal.* **2020**, *389*, 140−149.
(22) Paolucci, C.; Verma, A. A.; Bates, S. A.; Kispersky, V. F.; Miller, J. T.; Gounder, R.; Delgass, W. N.; Ribeiro, F. H.; Schneider, W. F. Isolation of the copper redox steps in the standard selective catalytic reduction on Cu-SSZ-13. *Angew. Chem., Int. Ed.* **2014**, *53* (44), 11828−33.
(23) Kwak, J. H.; Lee, J. H.; Burton, S. D.; Lipton, A. S.; Peden, C. H.; Szanyi, J. A common intermediate for N_2 formation in enzymes and zeolites: side-on Cu-nitrosyl complexes. *Angew. Chem., Int. Ed.* **2013**, *52* (38), 9985−9.
(24) Gramigni, F.; Nasello, N. D.; Usberti, N.; Iacobone, U.; Selleri, T.; Hu, W.; Liu, S.; Gao, X.; Nova, I.; Tronconi, E. Transient Kinetic Analysis of Low-Temperature NH_3-SCR over Cu-CHA Catalysts Reveals a Quadratic Dependence of Cu Reduction Rates on Cu^{II}. *ACS Catal.* **2021**, *11* (8), 4821−4831.
(25) Usberti, N.; Gramigni, F.; Nasello, N. D.; Iacobone, U.; Selleri, T.; Hu, W.; Liu, S.; Gao, X.; Nova, I.; Tronconi, E. An experimental and modelling study of the reactivity of adsorbed NH_3 in the low temperature NH_3-SCR reduction half-cycle over a Cu-CHA catalyst. *Appl. Catal., B* **2020**, *279*, 119397.
(26) Villamaina, R.; Liu, S. J.; Nova, I.; Tronconi, E.; Ruggeri, M. P.; Collier, J.; York, A.; Thompsett, D. Speciation of Cu Cations in Cu-CHA Catalysts for NH_3-SCR: Effects of SiO_2/AlO_3 Ratio and Cu-Loading Investigated by Transient Response Methods. *ACS Catal.* **2019**, *9* (10), 8916−8927.
(27) Villamaina, R.; Iacobone, U.; Nova, I.; Ruggeri, M. P.; Collier, J.; Thompsett, D.; Tronconi, E. Low-T CO Oxidation over Cu−CHA Catalysts in Presence of NH_3: Probing the Mobility of Cu^{II} Ions and the Role of Multinuclear Cu^{II} Species. *ChemCatChem.* **2020**, *12* (15), 3843−3848.
(28) Hu, W.; Iacobone, U.; Gramigni, F.; Zhang, Y.; Wang, X.; Liu, S.; Zheng, C.; Nova, I.; Gao, X.; Tronconi, E. Unraveling the Hydrolysis of Z_2Cu^{2+} to $ZCu^{2+}(OH)^-$ and Its Consequences for the Low-Temperature Selective Catalytic Reduction of NO on Cu-CHA Catalysts. *ACS Catal.* **2021**, *11* (18), 11616−11625.
(29) Ohata, Y.; Kubota, H.; Toyao, T.; Shimizu, K.; Ohnishi, T.; Moteki, T.; Ogura, M. Kinetic and spectroscopic insights into the behaviour of Cu active site for NH_3-SCR over zeolites with several topologies. *Catal. Sci. Technol.* **2021**, *11* (8), 2718−2733.
(30) Lomachenko, K. A.; Borfecchia, E.; Negri, C.; Berlier, G.; Lamberti, C.; Beato, P.; Falsig, H.; Bordiga, S. The Cu-CHA deNOx Catalyst in Action: Temperature-Dependent NH_3-Assisted Selective Catalytic Reduction Monitored by Operando XAS and XES. *J. Am. Chem. Soc.* **2016**, *138* (37), 12025−8.
(31) Gunter, T.; Carvalho, H. W.; Doronkin, D. E.; Sheppard, T.; Glatzel, P.; Atkins, A. J.; Rudolph, J.; Jacob, C. R.; Casapu, M.; Grunwaldt, J. D. Structural snapshots of the SCR reaction mechanism on Cu-SSZ-13. *Chem. Commun. (Camb)* **2015**, *51* (44), 9227−30.
(32) Luo, J.; Gao, F.; Kamasamudram, K.; Currier, N.; Peden, C. H. F.; Yezerets, A. New insights into Cu/SSZ-13 SCR catalyst acidity. Part I: Nature of acidic sites probed by NH_3 titration. *J. Catal.* **2017**, *348*, 291−299.
(33) Andersen, C. W.; Borfecchia, E.; Bremholm, M.; Jorgensen, M. R. V.; Vennestrom, P. N. R.; Lamberti, C.; Lundegaard, L. F.; Iversen, B. B. Redox-Driven Migration of Copper Ions in the Cu-CHA Zeolite as Shown by the In Situ PXRD/XANES Technique. *Angew. Chem., Int. Ed.* **2017**, *56* (35), 10367−10372.
(34) Janssens, T. V. W.; Falsig, H.; Lundegaard, L. F.; Vennestrom, P. N. R.; Rasmussen, S. B.; Moses, P. G.; Giordanino, F.; Borfecchia, E.; Lomachenko, K. A.; Lamberti, C.; Bordiga, S.; Godiksen, A.; Mossin, S.; Beato, P. A Consistent Reaction Scheme for the Selective

https://doi.org/10.1021/acscatal.2c01213
ACS Catal. 2022, 12, 5263−5274

Catalytic Reduction of Nitrogen Oxides with Ammonia. *ACS Catal.* **2015**, *5* (5), 2832−2845.
(35) Szanyi, J.; Kwak, J. H.; Zhu, H.; Peden, C. H. Characterization of Cu-SSZ-13 NH_3 SCR catalysts: an in situ FTIR study. *Phys. Chem. Chem. Phys.* **2013**, *15* (7), 2368−80.
(36) Lezcano-Gonzalez, I.; Wragg, D. S.; Slawinski, W. A.; Hemelsoet, K.; Van Yperen-De Deyne, A.; Waroquier, M.; Van Speybroeck, V.; Beale, A. M. Van Speybroeck, V.; Beale, A. M., Determination of the Nature of the Cu Coordination Complexes Formed in the Presence of NO and NH_3 within SSZ-13. *J. Phys. Chem. C* **2015**, *119* (43), 24393−24403.
(37) Zhang, R. Q.; McEwen, J. S.; Kollar, M.; Gao, F.; Wang, Y. L.; Szanyi, J.; Peden, C. H. F. NO Chemisorption on Cu/SSZ-13: A Comparative Study from Infrared Spectroscopy and DFT Calculations. *ACS Catal.* **2014**, *4* (11), 4093−4105.
(38) Goltl, F.; Sautet, P.; Hermans, I. Can Dynamics Be Responsible for the Complex Multipeak Infrared Spectra of NO Adsorbed to Copper(II) Sites in Zeolites? *Angew. Chem., Int. Ed.* **2015**, *54* (27), 7799−7804.
(39) Hu, W.; Zou, R.; Dong, Y.; Zhang, S.; Song, H.; Liu, S.; Zheng, C.; Nova, I.; Tronconi, E.; Gao, X. Synergy of vanadia and ceria in the reaction mechanism of low-temperature selective catalytic reduction of NOx by NH_3. *J. Catal.* **2020**, *391*, 145−154.
(40) Ruggeri, M. P.; Selleri, T.; Colombo, M.; Nova, I.; Tronconi, E. Identification of nitrites/HONO as primary products of NO oxidation over Fe-ZSM-5 and their role in the Standard SCR mechanism: A chemical trapping study. *J. Catal.* **2014**, *311*, 266−270.
(41) Ruggeri, M. P.; Selleri, T.; Colombo, M.; Nova, I.; Tronconi, E. Investigation of NO_2 and NO interaction with an Fe-ZSM-5 catalyst by transient response methods and chemical trapping techniques. *J. Catal.* **2015**, *328*, 258−269.
(42) Weiss, B. M.; Caldwell, K. B.; Iglesia, E. NOx Interactions with Dispersed BaO: Adsorption Kinetics, Chemisorbed Species, and Effects of Oxidation Catalyst Sites. *J. Phys. Chem. C* **2011**, *115* (14), 6561−6570.
(43) Schneider, W. F. Qualitative differences in the adsorption chemistry of acidic (CO_2, SOx) and Amphiphilic (NOx) species on the alkaline earth oxides. *J. Phys. Chem. B* **2004**, *108* (1), 273−282.
(44) Selleri, T.; Gramigni, F.; Nova, I.; Tronconi, E. NO oxidation on Fe- and Cu-zeolites mixed with BaO/Al_2O_3: Free oxidation regime and relevance for the NH_3-SCR chemistry at low temperature. *Appl. Catal., B* **2018**, *225*, 324−331.
(45) Selleri, T.; Ruggeri, M. P.; Nova, I.; Tronconi, E. The Low Temperature Interaction of NO+O_2 with a Commercial Cu-CHA Catalyst: A Chemical Trapping Study. *Top. Catal.* **2016**, *59* (8−9), 678−685.
(46) Hu, W.; Zhang, Y.; Liu, S.; Zheng, C.; Gao, X.; Nova, I.; Tronconi, E. Improvement in activity and alkali resistance of a novel V-$Ce(SO_4)_2$/Ti catalyst for selective catalytic reduction of NO with NH_3. *Appl. Catal., B* **2017**, *206*, 449−460.
(47) O'Malley, A. J.; Sarwar, M.; Armstrong, J.; Catlow, C. R. A.; Silverwood, I. P.; York, A. P. E.; Hitchcock, I. Comparing ammonia diffusion in NH_3-SCR zeolite catalysts: a quasielastic neutron scattering and molecular dynamics simulation study. *Phys. Chem. Chem. Phys.* **2018**, *20* (17), 11976−11986.
(48) Busca, G.; Lietti, L.; Ramis, G.; Berti, F. Chemical and mechanistic aspects of the selective catalytic reduction of NOx by ammonia over oxide catalysts: A review. *Appl. Catal., B* **1998**, *18* (1−2), 1−36.
(49) Zhu, M.; Lai, J. K.; Tumuluri, U.; Wu, Z.; Wachs, I. E. Nature of Active Sites and Surface Intermediates during SCR of NO with NH_3 by Supported V_2O_5-WO_3/TiO_2 Catalysts. *J. Am. Chem. Soc.* **2017**, *139* (44), 15624−15627.
(50) Song, I.; Lee, H.; Jeon, S. W.; Kim, D. H. Understanding the dynamic behavior of acid sites on TiO_2-supported vanadia catalysts via operando DRIFTS under SCR-relevant conditions. *J. Catal.* **2020**, *382*, 269−279.
(51) Marberger, A.; Ferri, D.; Elsener, M.; Krocher, O. The Significance of Lewis Acid Sites for the Selective Catalytic Reduction of Nitric Oxide on Vanadium-Based. *Catalysts. Angew. Chem. Int. Ed.* **2016**, *55* (39), 11989−94.
(52) Zhu, H.; Kwak, J. H.; Peden, C. H. F.; Szanyi, J. In situ DRIFTS-MS studies on the oxidation of adsorbed NH_3 by NOx over a Cu-SSZ-13 zeolite. *Catal. Today* **2013**, *205*, 16−23.
(53) Zhang, Y.; Peng, Y.; Li, K.; Liu, S.; Chen, J.; Li, J.; Gao, F.; Peden, C. H. F. Using Transient FTIR Spectroscopy to Probe Active Sites and Reaction Intermediates for Selective Catalytic Reduction of NO on Cu/SSZ-13 Catalysts. *ACS Catal.* **2019**, *9* (7), 6137−6145.
(54) Rizzotto, V.; Chen, D.; Tabak, B. M.; Yang, J. Y.; Ye, D.; Simon, U.; Chen, P. Spectroscopic identification and catalytic relevance of NH_4^+ intermediates in selective NOx reduction over Cu-SSZ-13 zeolites. *Chemosphere* **2020**, *250*, 126272.
(55) Jaegers, N. R.; Lai, J. K.; He, Y.; Walter, E.; Dixon, D. A.; Vasiliu, M.; Chen, Y.; Wang, C.; Hu, M. Y.; Mueller, K. T.; Wachs, I. E.; Wang, Y.; Hu, J. Z. Mechanism by which Tungsten Oxide Promotes the Activity of Supported V_2O_5/TiO_2 Catalysts for NOx Abatement: Structural Effects Revealed by (51) V MAS NMR Spectroscopy. *Angew. Chem., Int. Ed.* **2019**, *58* (36), 12609−12616.
(56) Forzatti, P.; Nova, I.; Tronconi, E. Enhanced NH_3 selective catalytic reduction for NOx abatement. *Angew. Chem., Int. Ed.* **2009**, *48* (44), 8366−8.
(57) Song, I.; Lee, H.; Jeon, S. W.; Kim, T.; Kim, D. H. Time-resolved observation of V_2O_5/TiO_2 in NH_3-SCR reveals the equivalence of Bronsted and Lewis acid sites. *Chem. Commun. (Camb)* **2020**, *56* (98), 15450−15453.
(58) Hun Kwak, J.; Zhu, H.; Lee, J. H.; Peden, C. H.; Szanyi, J. Two different cationic positions in Cu-SSZ-13? *Chem. Commun. (Camb)* **2012**, *48* (39), 4758−60.
(59) Gao, F.; Washton, N. M.; Wang, Y. L.; Kollar, M.; Szanyi, J.; Peden, C. H. F. Effects of Si/Al ratio on Cu/SSZ-13 NH_3-SCR catalysts: Implications for the active Cu species and the roles of Bronsted acidity. *J. Catal.* **2015**, *331*, 25−38.
(60) Ma, L.; Cheng, Y.; Cavataio, G.; McCabe, R. W.; Fu, L.; Li, J. Characterization of commercial Cu-SSZ-13 and Cu-SAPO-34 catalysts with hydrothermal treatment for NH_3-SCR of NOx in diesel exhaust. *Chem. Eng. J.* **2013**, *225*, 323−330.
(61) Da Costa, P.; Modén, B.; Meitzner, G. D.; Lee, D. K.; Iglesia, E. Spectroscopic and chemical characterization of active and inactive Cu species in NO decomposition catalysts based on Cu-ZSM5. *Phys. Chem. Chem. Phys.* **2002**, *4* (18), 4590−4601.
(62) Li, H.; Paolucci, C.; Khurana, I.; Wilcox, L.; Goltl, F.; Albarracin-Caballero, J. D.; Shih, A. J.; Ribeiro, F. H.; Gounder, R.; Schneider, W. F. Consequences of exchange-site heterogeneity and dynamics on the UV-visible spectrum of Cu-exchanged SSZ-13. *Chem. Sci.* **2019**, *10* (8), 2373−2384.
(63) Paolucci, C.; Di Iorio, J. R.; Schneider, W. F.; Gounder, R. R., Solvation and Mobilization of Copper Active Sites in Zeolites by Ammonia: Consequences for the Catalytic Reduction of Nitrogen Oxides. *Acc. Chem. Res.* **2020**, *53* (9), 1881−1892.
(64) Ravi, M.; Ranocchiari, M.; van Bokhoven, J. A. The Direct Catalytic Oxidation of Methane to Methanol-A Critical Assessment. *Angew. Chem., Int. Ed.* **2017**, *56* (52), 16464−16483.
(65) Ravi, M.; Sushkevich, V. L.; Knorpp, A. J.; Newton, M. A.; Palagin, D.; Pinar, A. B.; Ranocchiari, M.; van Bokhoven, J. A. Misconceptions and challenges in methane-to-methanol over transition-metal-exchanged zeolites. *Nat. Catal.* **2019**, *2* (6), 485−494.
(66) Pappas, D. K.; Borfecchia, E.; Dyballa, M.; Pankin, I. A.; Lomachenko, K. A.; Martini, A.; Signorile, M.; Teketel, S.; Arstad, B.; Berlier, G.; Lamberti, C.; Bordiga, S.; Olsbye, U.; Lillerud, K. P.; Svelle, S.; Beato, P. Methane to Methanol: Structure-Activity Relationships for Cu-CHA. *J. Am. Chem. Soc.* **2017**, *139* (42), 14961−14975.
(67) Newton, M. A.; Knorpp, A. J.; Pinar, A. B.; Sushkevich, V. L.; Palagin, D.; van Bokhoven, J. A. On the Mechanism Underlying the Direct Conversion of Methane to Methanol by Copper Hosted in Zeolites; Braiding Cu K-Edge XANES and Reactivity Studies. *J. Am. Chem. Soc.* **2018**, *140* (32), 10090−10093.

https://doi.org/10.1021/acscatal.2c01213
ACS Catal. 2022, 12, 5263−5274

(68) Dinh, K. T.; Sullivan, M. M.; Narsimhan, K.; Serna, P.; Meyer, R. J.; Dinca, M.; Roman-Leshkov, Y. Continuous Partial Oxidation of Methane to Methanol Catalyzed by Diffusion-Paired Copper Dimers in Copper-Exchanged Zeolites. *J. Am. Chem. Soc.* **2019**, *141* (29), 11641−11650.
(69) Di Iorio, J. R.; Hoffman, A. J.; Nimlos, C. T.; Nystrom, S.; Hibbitts, D.; Gounder, R. Mechanistic origins of the high-pressure inhibition of methanol dehydration rates in small-pore acidic zeolites. *J. Catal.* **2019**, *380*, 161−177.
(70) Chen, P.; Rizzotto, V.; Khetan, A.; Xie, K.; Moos, R.; Pitsch, H.; Ye, D.; Simon, U. Mechanistic Understanding of Cu-CHA Catalyst as Sensor for Direct NH_3-SCR Monitoring: The Role of Cu Mobility. *ACS Appl. Mater. Interfaces* **2019**, *11* (8), 8097−8105.
(71) Chen, P.; Khetan, A.; Jabłońska, M.; Simböck, J.; Muhler, M.; Palkovits, R.; Pitsch, H.; Simon, U. Local dynamics of copper active sites in zeolite catalysts for selective catalytic reduction of NOx with NH_3. *Appl. Catal., B* **2018**, *237*, 263−272.
(72) Wang, M.; Jaegers, N. R.; Lee, M. S.; Wan, C.; Hu, J. Z.; Shi, H.; Mei, D.; Burton, S. D.; Camaioni, D. M.; Gutierrez, O. Y.; Glezakou, V. A.; Rousseau, R.; Wang, Y.; Lercher, J. A. Genesis and Stability of Hydronium Ions in Zeolite Channels. *J. Am. Chem. Soc.* **2019**, *141* (8), 3444−3455.
(73) Feng, Y.; Janssens, T. V. W.; Vennestrøm, P. N. R.; Jansson, J.; Skoglundh, M.; Grönbeck, H. The Role of H^+- and Cu^+-Sites for N_2O Formation during NH_3-SCR over Cu-CHA. *J. Phys. Chem. C* **2021**, *125* (8), 4595−4601.
(74) Han, J.; Wang, A.; Isapour, G.; Härelind, H.; Skoglundh, M.; Creaser, D.; Olsson, L. N_2O Formation during NH_3-SCR over Different Zeolite Frameworks: Effect of Framework Structure, Copper Species, and Water. *Ind. Eng. Chem. Res.* **2021**, *60* (49), 17826−17839.
(75) Lin, F.; Andana, T.; Wu, Y.; Szanyi, J.; Wang, Y.; Gao, F. Catalytic site requirements for N_2O decomposition on Cu-, Co-, and Fe-SSZ-13 zeolites. *J. Catal.* **2021**, *401*, 70−80.
(76) Negahdar, L.; Omori, N. E.; Quesne, M. G.; Frogley, M. D.; Cacho-Nerin, F.; Jones, W.; Price, S. W. T.; Catlow, C. R. A.; Beale, A. M. Elucidating the Significance of Copper and Nitrate Speciation in Cu-SSZ-13 for N_2O Formation during NH_3-SCR. *ACS Catal.* **2021**, *11* (21), 13091−13101.
(77) Shih, A. J.; González, J. M.; Khurana, I.; Ramírez, L. P.; Peña L, A.; Kumar, A.; Villa, A. L. Influence of ZCuOH, Z_2Cu, and Extraframework CuxOy Species in Cu-SSZ-13 on N_2O Formation during the Selective Catalytic Reduction of NOx with NH_3. *ACS Catal.* **2021**, *11* (16), 10362−10376.
(78) Xi, Y.; Ottinger, N. A.; Keturakis, C. J.; Liu, Z. G. Dynamics of low temperature N_2O formation under SCR reaction conditions over a Cu-SSZ-13 catalyst. *Appl. Catal., B* **2021**, *294*, 120245.
(79) Yao, D.; Liu, B.; Wu, F.; Li, Y.; Hu, X.; Jin, W.; Wang, X. N_2O Formation Mechanism During Low-Temperature NH_3-SCR over Cu-SSZ-13 Catalysts with Different Cu Loadings. *Ind. Eng. Chem. Res.* **2021**, *60* (28), 10083−10093.

https://doi.org/10.1021/acscatal.2c01213
ACS Catal. 2022, 12, 5263−5274